JOURNAL OF MATERIALS SCIENCE 15 (1980) 3025–3035

Interactions between sulphur and microstructural defects in a Ni–16 wt% Cr–7 wt% Fe alloy and microsulphide nucleation

G. MOULIN, M. AUCOUTURIER, P. LACOMBE
Laboratoire de Métallurgie Physique, associé au CNRS No 177, Bât. 413 Université Paris-Sud, 91405 Orsay Cedex, France

The distribution of sulphur in the form of isolated atoms or microscopic sulphide particles (microsulphides) in the structure of two Inconel 600 alloys of different purity was analysed with the help of two new techniques: high-resolution sulphur autoradiography (with $^{35}S^{*}$) for the segregation of sulphur and high-resolution sulphur microprint to observe large amounts of sulphur. Among the various places where sulphur may segregate (grain boundaries, microprecipitates, slip-planes, isolated dislocations) some are preferred sites for further nucleation and growth of microsulphides. As a result, preferential interactions may be observed between sulphur and chromium oxycarbides, especially in the case of industrial alloys, in as much as they have a higher carbon content. The results have been considered essentially in terms of: (i) a gain in energy during the chemical reaction, which leads to the formation of chromium sulphides from chromium carbides and (ii) a reduction in overcrowding through the formation of microsulphides. The critical free energy W^{*} for the nucleation of microsulphide is considered with the help of the Burke equation.

1. Introduction

Nickel-base alloys, such as Inconel 600, used as heat-exchanger tube matrices in Pressurized Steam-Generating Nuclear Stations, are particularly susceptible to sulphur pollution in H_2/H_2S gas. In an earlier study the presence of chromium sulphides in the metal at a depth of 300 to 350 μm for sulphurization time of 8 h at 1000° C under a pressure $PH_2S = 6 \times 10^{-2}$ atm (with PH_2 = 0.25 atm) [1] was noted. Many authors consider that the brittleness of the metal is, in fact, linked to small amounts of sulphur in the form of isolated atoms or small clusters of atoms [2, 3]. It is now possible to localize the position of the sulphur within the microstructure with the help of two new techniques: high-resolution sulphur autoradiography (HRA with ^{35}S) to observe the segregation of sulphur in the form of isolated atoms [4, 5] and high-resolution sulphur microprint† to detect larger quantities of atoms which might lead to the formation of microscopic sulphide particles (microsulphides) [6].

The first technique has already shown, by scanning electron microscopy (SEM) a preferential localization of sulphur immediately above the intergranular chromium carbides, especially in the case of industrial alloys, in as much as they have a higher carbon content (Fig. 1). Such intergranular interactions greatly alter the mobility of the sulphur and lead to great variations in the sulphur grain-boundary mobility factor ($D_j\delta$) with respect to the purity or the microstructural shape of the alloys, or with the temperature (a notable decrease in the $D_j\delta$ values is seen at temperatures where the intergranular carbides dissolve in the matrix [4]).

The present paper is a more detailed study by transmission electron microscopy (TEM) of the various preferred sites of sulphur atoms on grain

†Or "Baumann microprint".

0022–2461/80/123025–11$03.10/0

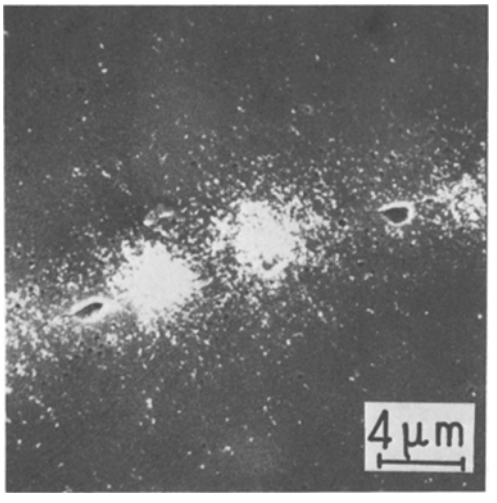

Figure 1 Pure alloy in a desensitized state. Distribution of silver filaments above the intergranular chromium oxy-carbides.

boundaries as well as on linear and planar defects (e.g. internal twins, slip lines, dislocation lines, isolated dislocations, twin boundaries, precipitates). In this work, using the high-resolution sulphur microprint, the most favourable sites for further nucleation of the chromium sulphides, both in the case of pure alloys and in the case of industrial alloys, will be analysed.

2. Materials and experimental procedure

The materials are two kinds of Inconel 600 alloy of different purities: an impure alloy of industrial origin, the chemical composition of which is given in Table I, and a pure alloy, prepared at the Ecole des Mines de St-Etienne, with 0.003 wt % C, 0.020 wt % O and 0.002 wt % N. The samples, in the form of foils 0.12 to 0.15 mm thick are subjected to the treatment presented in Fig. 2.

2.1. Heat-treatment

2.1.1. Previous heat-treatment

Heat-treatment is carried out in a quartz capsule sealed in an argon atmosphere, followed by quenching to -70° C (in a CO_2–alcohol mixture). The homogenizing treatment, which lasts 70 h at 1150° C, is followed by a tempering treatment of

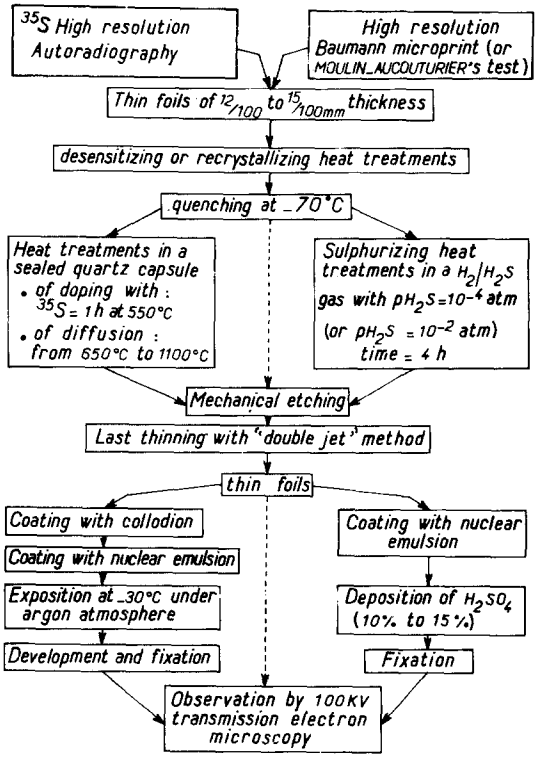

Figure 2 Experimental procedure.

either an "intergranular corrosion desensitizing treatment" lasting 16 h at 700° C followed by quenching (this gives the grain boundary precipitates a globular shape and suppresses the chromium gradient near the grain boundaries), or a recrystallizing treatment of 16 h at 700° C, followed by quenching, 60% cold rolling and 72 h at 800° C, then another quench.

2.1.2. Further heat-treatment

The ^{35}S diffusion treatment is also carried out in sealed quartz capsules at temperatures between 650 and 1100° C. These are preceded by ^{35}S deposition lasting 1 h at 550° C. The total quantity of sulphur which enters the material is much less than 0.05 mg; it can therefore be considered as a penetration of sulphur in the form of isolated atoms. The sulphuration heat-treatment takes place in a H_2/H_2S atmosphere with H_2S pressure of 10^{-4} atm (with $P_{H_2} = 0.25$ atm) for 4 h [1].

TABLE I Chemical composition of impure alloys (in wt %)

C	Si	Mn	S	P	Cr	Ni	Co	Ti	Cu	Al	Fe
0.025	0.32	0.78	0.003	0.009	16.20	73.65	0.04	0.19	< 0.01	0.11	8.47

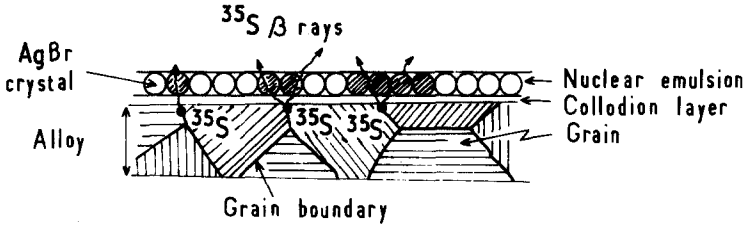

Figure 3 High-resolution sulphur autoradiography.

2.2. Sample thinning

Samples 0.12 to 0.15 mm thick are thinned by the double-jet technique in an aceto-perchloric bath (950 ml : 50 ml) with a voltage of 70 mV, a current of 0.12 mA and a temperature of 17° C. In the thinnest part of the foil the depth in relation to the original surface is approximately 60–70 μm, which is the beginning of the intergranular diffusion zone.

2.3. Autoradiography

The thin foils are coated with a thin monolayer of AgBr grains (Ilford L4 emulsion), with an approximate size of 1400 Å.

In the case of high-resolution sulphur autoradiography (with ^{35}S), the surface of the specimens is pre-coated with a thin layer of collodion as represented in Fig. 3. Irradiation takes place under a purified argon atmosphere at − 30° C to avoid any risk of oxidation. The autoradiographic image, after activation of AgBr by ^{35}S β-emission development (D_{19} B developer) and fixing, appears as black silver filaments [4–6].

In the case of the high-resolution sulphur microprint, the AgBr layer is covered with a thin aqueous film of sulfuric acid (H_2SO_4 10 to 15 vol%). The silver from the AgBr in the nuclear emulsion interacts chemically with the H_2S to form silver sulphide, Ag_2S (Fig. 4). The chemical interactions are of the following kinds in the case of CrS,

$$H_2SO_4 + CrS \rightarrow H_2S_{(g)} + Cr(SO_4)$$

and

$$H_2S_{(g)} + 2AgBr \rightarrow Ag_2S_{(s)} + 2HBr$$

Simple fixing is then necessary to isolate the Ag_2S particles, which appear as black spheres under the transmission electron microscope [7].

3. Microstructural study

The microstructure of the specimens will now be described, with the help of the transmission electron microscope after the same heat-treatment as used in sulphuration; in this study tempering is carried out in a hydrogen or argon atmosphere, without a H_2S or sulphur atmosphere.

3.1. Microstructure after "desensitizing treatment"

The microstructure has an austenitic shape with grains of heterogeneous sizes, between 100 and 500 μm diameter.

The grain boundaries of the pure specimens are almost free of precipitate (Fig. 5). Chromium oxycarbides may be observed either at the "triple points" or at the points where the slip-planes come into contact with the grain boundaries. Dislocations are very common in the latter case. On the other hand, carbides are very numerous in the grain boundaries of the impure alloys and appear adjacent to many precipitates of different oxides (e.g. Cr_2O_3, $NiCr_2O_4$, Fe_3O_4) (Table II).

The morphology of the precipitates changes with the tempering temperature. At the lowest temperatures (~ 650° C), the chromium carbides ($Cr_{23}C_6$) and the oxides are small in size and are not only concentrated in the grain boundaries but also may be found on either side of some of the

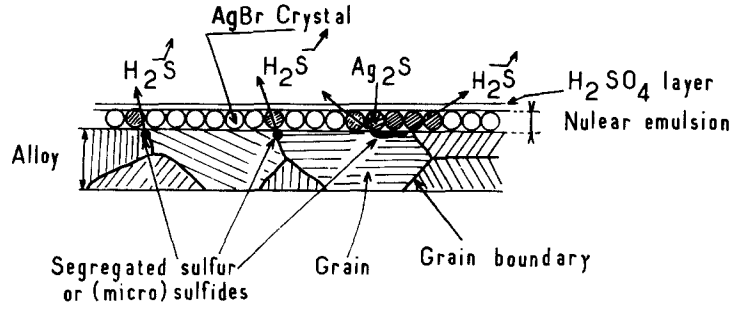

Figure 4 High-resolution Baumann microprint.

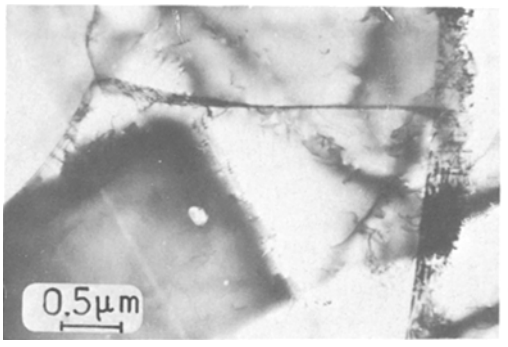

Figure 5 Microstructure of pure alloy after desensitizing treatment at 650° C (note that the grain boundaries are free from precipitates).

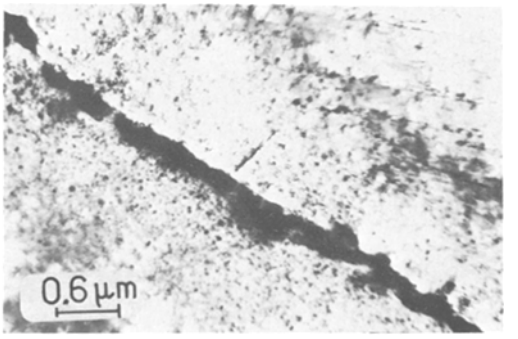

Figure 6 Morphology of a grain boundary in the case of an impure alloy after desensitizing treatment at 650° C.

boundaries. These precipitates decrease in size and density according to their distance from the boundary (Fig. 6). At the higher temperatures, the $Cr_{23}C_6$ precipitates become more globular and a maximum size is reached at 900 to 950° C (Fig. 7). A high density of dislocations may be seen around these precipitates. When the carbides dissolve in the matrix (at 950–1000° C), essentially only the oxides (Cr_2O_3, $NiCr_2O_4$, Fe_3O_4 or Fe_2O_3) subsist in the grain boundaries (Table II).

In the coarse grains some defects may be observed in addition to the great number of carbides, oxides, nitrides or even sulphides (Table II). These include twins of (1 1 1)[1 1 2] type (Fig. 5), dislocation lines, decorated with atoms of carbon or with microcarbides of $Cr_{23}C_6$ [8], especially at the lowest temperature of 650° C and slip-planes {1 1 1}, particularly after ^{35}S diffusion, tempering or sulphidizing heat-treatment in H_2/H_2S gas.

3.2. Recrystallization heat-treatment

The grain size in recrystallization heat-treatment is also quite heterogeneous, with an average diameter smaller than in the desensitized specimens, 50 to

TABLE II Leading precipitates in pure and impure alloys of Inconel 600 (identified by TEM according to the American Society for the Testing of Metals card-index).

Microstructural form		Area	Heat treatments		
			Desensitized	Desensitized + 5 days at 660° C or + 3 days at 800° C or + 1.5 days at 900° C	Desensitized + 3 h at 1000° C
Pure alloy	Desensitized	Grain boundaries	$Cr_{23}C_6$	$Cr_{23}C_6$	–
		Bulk	some oxycarbides and some Cr_2O_3	some oxycarbides and some Cr_2O_3	some Cr_2O_3
	Recrystallized	Grain boundaries	$Cr_{23}C_6$ + CrN	$Cr_{23}C_6$ + CrN	–
		Bulk	some oxycarbides and some Cr_2O_3	some oxycarbides and some Cr_2O_3	some Cr_2O_3
Impure alloy	Desensitized	Grain boundaries	$Cr_{23}C_6$ + some TiC + some oxycarbides	$Cr_{23}C_6$ + some TiC + some oxides	some TiC + some oxides
		Bulk	$Cr_{23}C_6$ + oxides (Fe, Ni or Cr) + TiC	$Cr_{23}C_6$ + oxides (Fe, Si, Ni or Ti, Cr, Mn) + TiC	oxides (Cr, Fe, Ni, Ti)
	Recrystallized	Grain boundaries	$Cr_{23}C_6$ + some TiC + some oxides	$Cr_{23}C_6$ + Fe_3MoC + Cr_3Nb_3C + some TiC + some oxides	some oxides (Fe, Cr, Ni)
		Bulk	oxides (Ni, Cr, Fe, Al, Mg, Ti) + $Cr_{23}C_6$ + TiC	oxides (Ni, Cr, Fe, Al, Mg, Ti) + $Cr_{23}C_6$ + TiC	oxides (Ni, Fe, Cr) + Ni_3N + Fe_3N

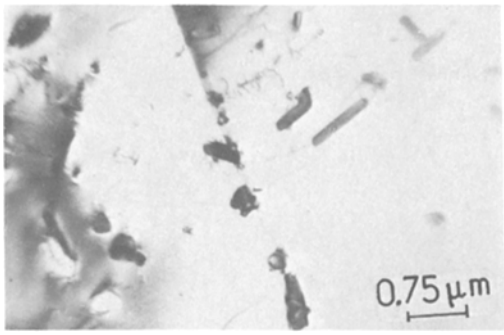

Figure 7 Microstructure of an impure alloy after tempering at 900° C.

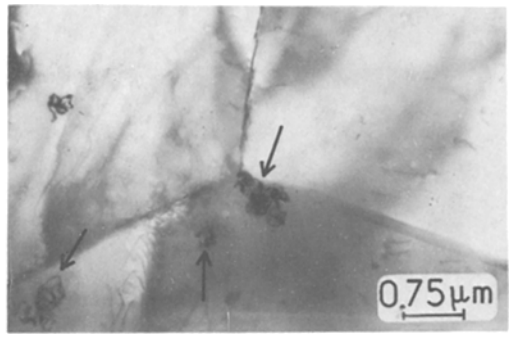

Figure 9 Localization of silver filaments on triple-points. Pure alloy in a desensitized state after sulphidizing treatment at 650° C. High-resolution autoradiography with $^{35}S^*$.

100 µm, in the case of pure alloys [1] and 10 to 20 µm, in the case of impure alloys [1].

When the specimens are pure, the grain boundaries are quite free from precipitation. Two kinds of grain boundaries may be distinguished in the case of the impure alloys. Some alloys are marked by alignments of chromium carbides $Cr_{23}C_6$. It is conceivable that the intergranular carbides, formed after the first desensitizing treatment, remain in the same place during rolling and recrystallizing treatment and prevent some recrystallizing grain boundaries from moving. Other boundaries are much more free of carbide precipitation (Fig. 8).

Dislocations are often arranged as slip lines and in great numbers, particularly near grain boundaries in pure alloys. Recrystallization heat-treatment produces a much greater number of linear defects than "desensitizing heat-treatment".

The intragranular chromium carbides or oxides tend to be concentrated all along the defects. In impure alloys the $Cr_{23}C_6$ carbides – which have a globular shape at 900° C – often contain Fe, Nb and Mo. In the case of pure specimens, chromium nitride (CrN) may also be identified after recrystallizing treatment (Table II).

4. Autoradiographic study

4.1. Pure alloys

4.1.1. Sulphur segregation of atoms in the elementary state

On autoradiographs exposed after the "desensitizing heat-treatment" and the sulphidizing treatment, silver filaments showing atomic sulphur are visible on the grain boundaries, particularly on "triple points" (Fig. 9), or in the vicinity of the rare intergranular $Cr_{23}C_6$ precipitates (Fig. 10). After recrystallizing treatment, followed by sulphidizing treatment, interactions can be detected between sulphur and dislocations in the vicinity of the grain boundaries, so that the sulphur distribution looks more diffuse (Fig. 11). In the grain bulk, a large gathering of silver filaments can be observed on the slip lines, after the lowest sulphidizing temperatures of 650° C (Fig. 12). The sulphur also has

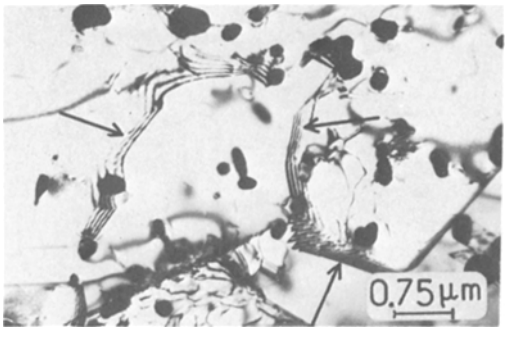

Figure 8 Microstructure of an impure alloy after recrystallizing treatment at 800° C (note that the sub-grain boundaries are relatively free from carbide precipitation).

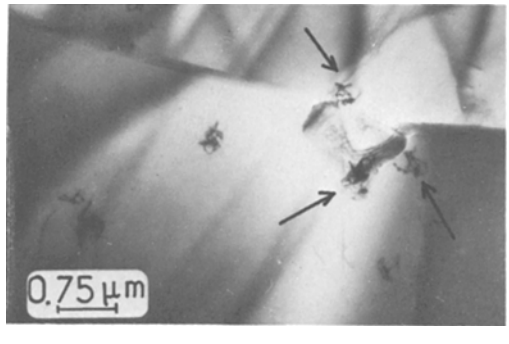

Figure 10 Sulphur segregation around a carbide in the grain boundaries. Pure alloy in a desensitized form after sulphidizing treatment at 650° C. High-resolution autoradiography with $^{35}S^*$.

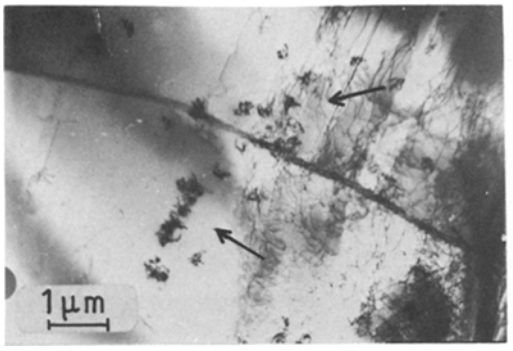

Figure 11 Interaction between sulphur and dislocations in the vicinity of a grain boundary in a pure recrystallized specimen ($T = 800°$ C). High-resolution autoradiography with $^{35}S^*$.

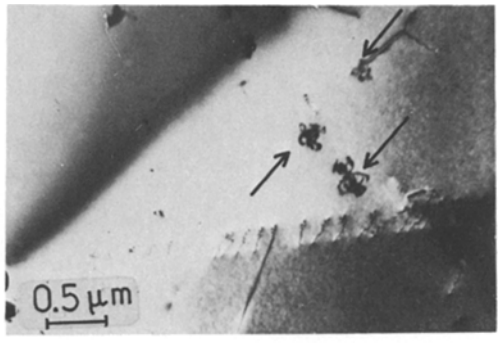

Figure 13 Segregation of sulphur above individual dislocations. Pure alloy recrystallized ($T = 650°$ C). High-resolution autoradiography with $^{35}S^*$.

a particular tendency to segregate above the isolated dislocations in the recrystallized specimens (Fig. 13).

When the sulphidization temperature is raised to 900° C, many places are then marked by sulphur e.g. the slip planes, the twin boundaries (Fig. 14) and the points where slip planes come into contact with the grain boundaries.

Of course, the localization of silver filaments on these different defects is always less accurate in the recrystallized specimens showing a great number of dislocations.

During the 1000° C sulphidizing treatment, the distribution of sulphur in atomic form is more random, though sulphur segregation may be seen immediately above some chromium oxide in the matrix.

4.1.2. *Chromium sulphide micro-precipitation*

The high-resolution sulphur microprint method confirms the main places for nucleation and growth of chromium microsulphides, shown by ^{35}S high resolution autoradiography. A certain number of Ag_2S black spheres may be observed on the grain boundaries (Fig. 15), but they may also be observed on the dislocation-lines marked by chromium micro-carbides at 650° C, on the slip-lines or at the points of contact with the grain boundaries (Fig. 16) and on the oxycarbides, which are near the slip-planes (Fig. 17).

4.2. Impure alloys

4.2.1. *Segregation of sulphur in atomic form*

After the desensitizing and sulphidizing treatments, the sulphur tends to settle along the grain boundaries as in pure alloys, but also, in the vicinity of the grain boundaries, on the slip-lines which are rich in microcarbides, as reported in Section 2.

The main difference from pure alloys is a selective silver filament mark on the numerous intergranular chromium carbides, excluding chromium

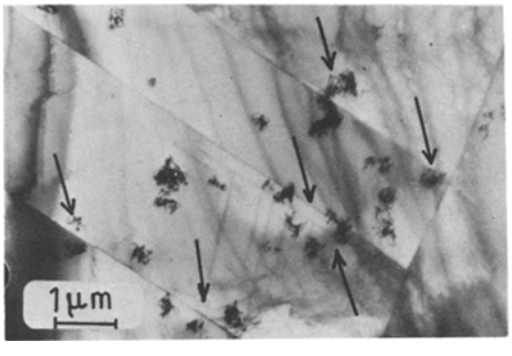

Figure 12 Localization of sulphur along the slip lines. Pure alloy, recrystallizing treatment at 650° C. High-resolution autoradiography with $^{35}S^*$.

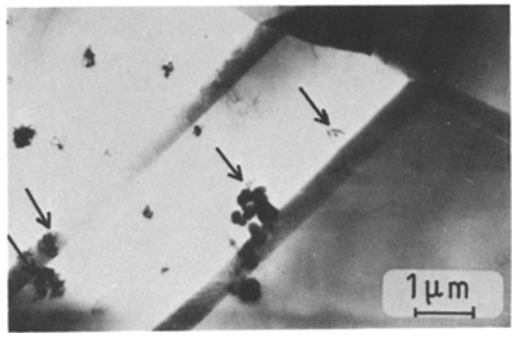

Figure 14 Silver filaments collecting in the twin boundaries of pure alloy, after desensitizing treatment at 800° C. High-resolution autoradiography with $^{35}S^*$.

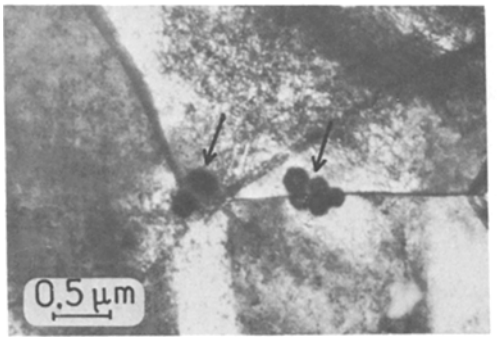

Figure 15 High-resolution sulphur microprint. Microsulphides on the grain boundaries. Pure alloy desensitized after sulphidizing treatment for 4 h at 650° C with a H_2S pressure of 10^{-4} atm.

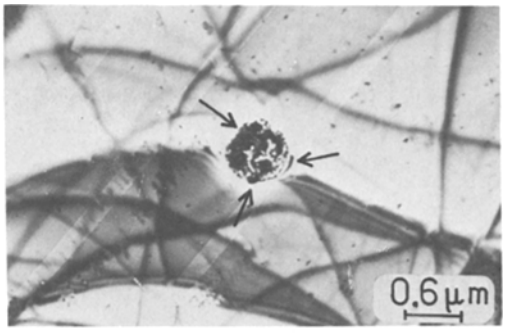

Figure 17 Ag_2S sulphur on an oxycarbide, near slip lines. Pure alloy desensitized after sulphidizing treatment of 4 h at 800° C.

oxides, even when they are alone in the grain boundaries at 1000° C. In recrystallized samples, sulphur also interacts with dislocations, whether regularly disposed or not, near the chromium carbides (Fig. 18).

In the matrix, when the sulphidizing temperatures are low, approximately 650° C, the different defects already quoted (slip-planes, twin-boundaries, etc.) are also possible places for sulphur deposition, along with chromium carbides, as in pure alloys (Fig. 19). But when the sulphuration temperature is raised the precipitation becomes greater and sulphur is located particularly on intragranular carbides which mainly gather in the grains, along slip-planes or twin boundaries, in recrystallized specimens (Fig. 20). The extent of the intragranular precipitation of these chromium carbides may even lead to a more pronounced segregation of sulphur, in its elementary form, in the matrix of some grains, than in the grain boundaries themselves. At 1000° C, no particular places seem to exist for the localization of silver filaments. They appear with similar probability on the dislocations, the twins, and the various kinds of precipitate.

4.2.2. *Chromium microsulphide precipitation*

According to the high-resolution sulphur microprint, the $Cr_{23}C_6$ chromium carbides seem predisposed to receive the largest distribution of sulphur, particularly on dislocations in their vicinity or near the grain boundaries, principally in the desensitized, then 800° C-sulphidized, microstructure (Fig. 21).

After the recrystallizing and sulphidizing treatments, the microsulphides nucleate on the precipitates lying in the former "desensitizing heat-treatment" grain boundaries and on the dislocation lines (Fig. 22), as in the recrystallization sub-grain boundaries (Fig. 23). For the newly formed grain boundaries, which are purer with respect to precipitation, the results are the same as those

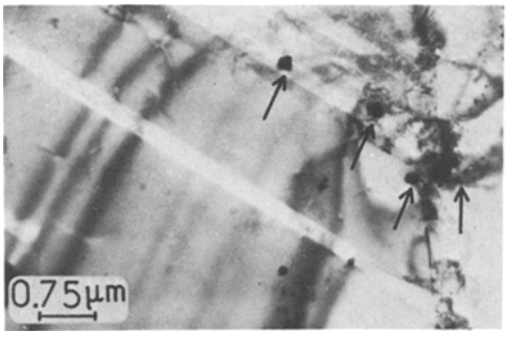

Figure 16 Microsulphides along the slip planes observed by high-resolution Baumann microprint. Pure alloy desensitized after sulphidizing treatment for 4 h at 800° C with a H_2S pressure of 10^{-4} atm.

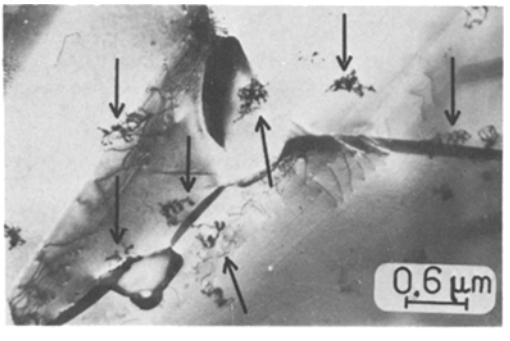

Figure 18 Silver filaments which segregate in a preferential manner in the dislocation near the intergranular carbides of a recrystallized impure alloy at 800° C. High-resolution sulphur autoradiography with $^{35}S^*$.

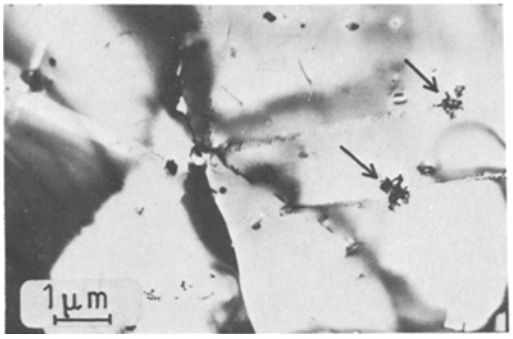

Figure 19 High-resolution sulphur autoradiography showing a segregation of sulphur on different defects in an impure alloy, recrystallized after sulphidizing treatment at 650° C.

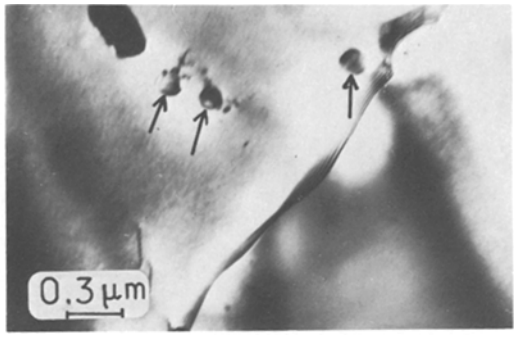

Figure 21 High-resolution sulphur microprint. Ag_2S spheres are located on the dislocations near the carbides. Impure alloy in a desensitized form, sulphidized for 4 h at 800° C.

obtained in the case of pure alloys. The black Ag_2S spheres are visible either on triple-points or on the points where twins and grain boundaries come into contact.

Likewise, in the matrix, the $Cr_{23}C_6$ chromium carbides are the favourite places for nucleation and growth of microsulphides, at temperatures below 1000° C (Fig. 21). At 1000° C, this role is played by the oxides (Fig. 24).

5. Discussion of the results

This study shows how the defects in the microstructures influence the distribution of sulphur in its elementary form, according to the temperature. The sulphur penetration in this kind of alloy is practically determined by the interaction of this element with all the defects already present in the microstructure, such as carbides, precipitates, twin planes, dislocations etc. This observation confirms the former results obtained on a macroscopic scale and mentioned in the first part of this paper. The preferential sites for the distribution of microsulphides, after sulphidization treatment under H_2/H_2S atmosphere, are the same as those for radioactive sulphur (^{35}S). They can be classified in the following manner: grain boundaries, intergranular carbides, area of contact of grain boundaries and slip lines, slip lines or twin boundaries and individual dislocations or dislocation lines marked by chromium microcarbides. The different critical energy for the formation of chromium sulphides can then be calculated in order to understand which are the preferred sites for nucleation and growth of the sulphides in the microstructure. Let us now postulate that the kinetics of the sulphur penetration and of the microsulphide formation are controlled by a solid-state diffusion process (Table III) [9].

Firstly, the values of the interfacial energies between matrix and precipitates, that is, γ_F, are computed with the help of the Ostwald analysis which relates the size variation of the precipitates to time and which appears in the Lifshitz–Wagner relation [10],

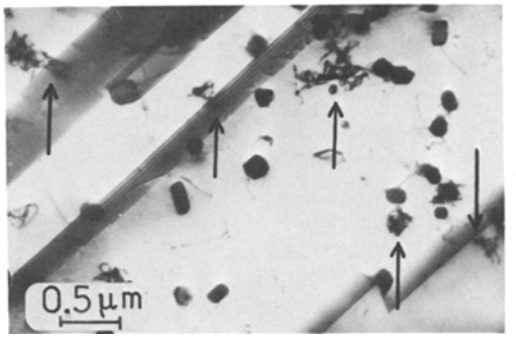

Figure 20 High-resolution sulphur autoradiography. Segregation of sulphur on the carbides along the slip planes in a recrystallized impure alloy. Sulphidizing treatment 4 h at 800° C.

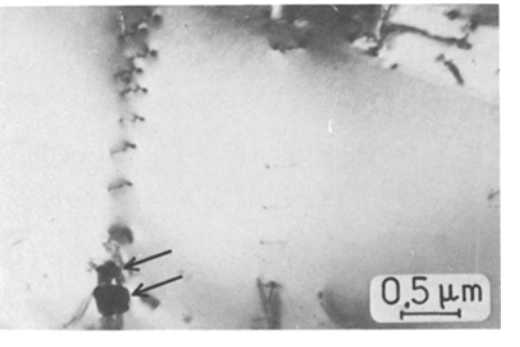

Figure 22 High-resolution sulphur microprint showing localization of Ag_2S spheres on the dislocation lines near a grain boundary. Impure alloy in a desensitized form, sulphidized for 4 h at 900° C.

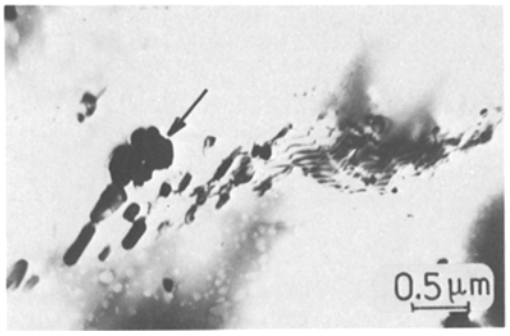

Figure 23 Ag_2S spheres near the carbides on a sub-grain boundary showing localization of microsulphides. Impure alloy in a recrystallized form, sulphidized for 4 h at 800° C.

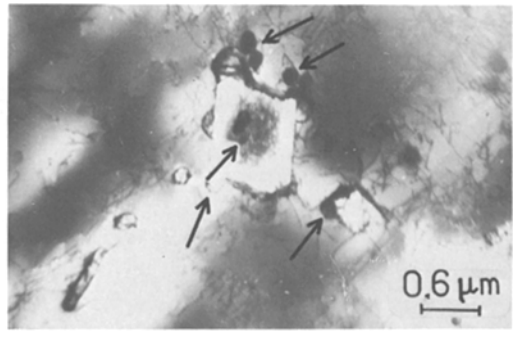

Figure 24 Microsulphides near the titanium oxides in the matrix of an impure alloy in a desensitized form after sulphidizing treatment for 4 h at 1000° C. High-resolution sulphur microprint.

$$r^3 - r_0^3 = \frac{8\gamma D C_e V_m^2}{9RT}(t - t_0) \qquad (1)$$

or

$$\gamma_F = \frac{9}{8}\frac{RT(r^3 - r_0^3)}{DC_e V_m^2 \Delta t}, \qquad (2)$$

where $r(r_0)$ is the mean precipitate radius, D is the chromium diffusion coefficient (Table III), V_m is the molar volume of the compound, γ is the precipitate interfacial energy, R is the gas constant and T is the temperature.

The different values of γ_F are presented in Table IV. At 650° C, the γ value is exceptionally high. If the chemical compositions of the alloy and of the embryos, and hence the values of ΔG for the formation of sulphides, remain unchanged, it becomes possible to calculate the critical free energy for sulphide nucleation, W^*, with the help of the Burke formula, which takes into account the stresses induced by precipitation [11]

$$W^* = \frac{8}{3}\frac{\pi^3 \mu^2 (\Delta)^4 \gamma^3}{(\Delta G_V)^4}, \qquad (3)$$

where μ is the matrix elastic shear modulus (8.4×10^{11} dyne cm^{-2}), Δ is the expansion coefficient associated with relative variation of matrix volume due to precipitation of new phase (e.g. 3.9 for $Cr \rightarrow Cr_2S_3$ [12]) and γ is the interfacial energy between matrix and precipitate

$$\Delta G_{(Cr \rightarrow CrS)} = +11\,795 - 13.24T \qquad (4)$$

(taking into account the dissociation of H_2S into S_2, then S_2 into atomic S [13]).

The different values of critical nucleation energy are presented in Table V.

Of course, there is a selective growth of chromium sulphides along grain boundaries where there is a preferential diffusion of chromium and sulphur. However, taking into account the exceptionaly high values of W^* at the lowest temperatures and the small values of chromium and sulphur diffusion coefficients (Table III), it is then possible to understand the importance of defects such as slip lines or planes, dislocations and twin boundaries, for chromium sulphide germination. Moreover, a high density of dislocations, after recrystallization heat-treatment, disturbs the sulphur distribution which is more diffuse in the area of the different defects already mentioned.

When the temperature is raised, the critical energies for nucleation become more compatible with the energy available through chromium sulphide formation. In fact linear defects are not the only ones to intervene, particularly in the case of impure alloys, where a pronounced precipitation of $Cr_{23}C_6$ can be seen from 800° C in the grain boundaries as well as in the matrix (the precipitates

TABLE III Diffusion coefficient of chromium and sulphur as a function of temperature

Diffusion coefficient in volume (D_v)	Temperature (°C)				Reference number
	650	800	900	1000	
D_vCr (cm^2 sec^{-1})	6×10^{-16}	3×10^{-14}	0.5×10^{-13}	6×10^{-12}	[9]
D_vS (cm^2 sec^{-1})	8×10^{-13}	6×10^{-12}	6×10^{-11}	5×10^{-10}	[4]

TABLE IV Calculated values of interfacial energies (γ_F) as a function of temperature

Interfacial energies	Temperature (° C)			
	650	800	900	1000
γ_F($\times 10^{-5}$ J cm^{-2})	125	30.0	9.00	2.50

TABLE VI ΔG for the formation of CrS from $Cr_{23}C_6$ or Cr_2O_3 as a function of temperature

Free energy ΔG(cal mol^{-1})	Temperature (° C)			
	650	800	900	1000
$Cr_{23}C_6 \rightarrow CrS$	− 425	− 2410	− 3740	− 5060
$Cr_2O_3 \rightarrow CrS$	3460	+ 22 500	+ 34 600	+ 48 440

are even located along the intergranular defects in the recrystallized state). The formation of sulphides from $Cr_{23}C_6$ carbides is more likely for many reasons: (i) Chromium activity in the carbides is much higher than in the matrix, the former are therefore preferred sites for chromium sulphide germination, (ii) The chemical reaction which leads, for instance, to the formation of CrS from $Cr_{23}C_6$ corresponds to a gain in energy but this is not the case with oxides (Table VI); (iii) The "overcrowding factor", Δ, also favours the formation of chromium sulphide, on the carbides in which the value of Δ is reduced to $\Delta_2 = 8.3 \times 10^{-2}$ instead of $\Delta_1 = 3.9$, for the formation of Cr_2S_3 from chromium [12] (i.e. a ratio $(\Delta_1)^4/(\Delta_2)^4$ of 10^{-7} in Equation 3).

Sulphide formation is restricted by carbide dissolution kinetics. The flow of matter which results from the dissolution of precipitate grain is expressed by [14]

$$-\frac{dm}{dt} = 4\pi R^2 D \left(\frac{d[Cr]}{dr}\right), \qquad (5)$$

where D is the chromium bulk diffusion coefficient, $(d[Cr]/dr)_R = (C - Cr/\delta)$ is the surface concentration gradient, C is the bulk concentration of the solution, [Cr] is the surface concentration of a precipitate grain and δ is the depth of the chromium gradient around the dissolving carbide grain.

The bulk diffusion coefficient of carbon is about a hundred times higher than that of sulphur, and carbide dissolution may easily take place. During the process, sulphur would then collect on the dislocations near the chromium carbides.

6. Conclusion

^{35}S high-resolution autoradiography and sulphur microprint (or Baumann microprint) techniques together enable the determination of preferred sites for sulphur accumulation in its elementary form, and for chromium sulphide nucleation and growth. The sulphur atoms tend to segregate along grain boundaries, particularly on the triple-points. However, the different microstructural points are possible sites for sulphur localization, i.e. slip lines or planes, twin boundaries. The inter- and transgranular carbides greatly modify the distribution of sulphur, especially in the case of impure alloys. After recrystallization tempering, the sulphur marks on the various transgranular $Cr_{23}C_6$ precipitates may appear even more numerous than the marks on the grain boundaries. In the same way, the dislocations, especially after cold rolling and recrystallization, are anchoring points for the sulphur atoms and give the sulphur distribution a more diffuse appearance in the vicinity of defects and grain boundaries. To justify the different sites for chromium sulphide nucleation and growth in relation to temperature, the following equation has been used, giving the critical nucleation free energy

$$W^* = \frac{8}{3}\frac{\pi^2\mu^2(\Delta)^4\gamma^3}{(\Delta G_V)^4}. \qquad (6)$$

We have considered the results as energetic gain (or reduction in overcrowding) during the formation of chromium sulphides from carbides. Thus at the lowest temperatures the growth of sulphides takes place essentially on slip lines etc., because of the energy contained in the defects. When the temperature is raised the nucleation of microsulphides is facilitated, but occurs preferentially on carbides owing to their high chromium content, and the energetic gain and reduction in overcrowding associated with chromium sulphide formation from carbides.

TABLE V Critical energies W^* for sulphides germination as a function of temperature

Critical energies	Temperature (° C)			
	650	800	900	1000
W^*(cal cm^{-3})	8.6×10^4	12.3	0.06	37×10^{-4}
W^*(cal mol^{-1})	1.5×10^6	212	1	6.3×10^{-3}

Acknowledgements

The authors would like to thank the Departement Etude des Matériaux, Direction des Etudes et des Recherches de l'Electricité de France, Les Renardières, for financial support and supply of materials.

References

1. G. MOULIN, M. AUCOUTURIER and P. LACOMBE, *J. Nucl. Mater.* **82** (1979) 347.
2. J. H. WESTBROOK and S. FLOREEN, *Can. Met. Quart.* **13** (1974) 181.
3. M. GUTTMANN, *Met. Sci.* **10** (1976) 337.
4. G. MOULIN, M. AUCOUTURIER and P. LACOMBE, *J. Nucl. Mater.* **82** (1979) 372.
5. J. P. LAURENT and G. LAPASSET, *J. Appl. Rad. and Isotopes* **24** (1973) 213.
6. A. M. HUNTZ, D. MARCHIVE, M. AUCOUTURIER and P. LACOMBE, *ibid.* **24** (1973) 689.
7. G. MOULIN, J. OVEJERO GARCIA, C. HAUT, M. DADIAN and M. AUCOUTURIER, *Rev. Mét.* **11** (1978) 627.
8. G. JOUVE, M. PATRICIU and M. AUCOUTURIER, *Corr. Sci.* **12** (1972) 537.
9. D. D. PRUTHI, M. S. ANAND and R. P. AGARWALA, *J. Nucl. Mater.* **64** (1977) 206.
10. J. M. LIFSHITZ and V. V. SLYOZOV, *J. Phys. Chem. Solids* **19** (1961) 35.
11. J. BURKE, "La cinétique des changements de phase dans les métaux" (Masson Edit., Paris, 1968) p. 149.
12. J. C. COLSON, M. LAMBERTIN and J. P. LARPIN, *Mém. Sci. Rev. Mét.* **11** (1977) 687.
13. F. D. RICHARDSON and J. H. E. JEFFES, *J. Iron and Steel Inst.* **6** (1952) 165.
14. B. MUTAFTSCHEV, H. CHAJES and R. GINDT, *Ed. CNRS* **152** (1965) 419.

Received 17 April and accepted 12 May 1980.